This article has been accepted for publication in a future issue of this journal, but has not been fully edited. Content may change prior to final publication. Citation information: DOI 10.1109/TCOMM.2017.2664866, IEEE Transactions on Communications

Degrees of Freedom of the Full-Duplex Asymmetric MIMO 3-Way Channel with Unicast and Broadcast Messages

Adel M. Elmahdy[1,6], Amr El-Keyi[1,2], Yahya Mohasseb[3], Tamer ElBatt[1,4], Mohammed Nafie[1,4], Karim G. Seddik[5], and Tamer Khattab[6]

[1]Wireless Intelligent Networks Center (WINC), Nile University, Giza, Egypt.
[2]Department of Systems and Computer Engineering, Carleton University, Ottawa, ON, Canada.
[3]Dept. of Communications, The Military Technical College, Cairo, Egypt.
[4]Dept. of EECE, Faculty of Engineering, Cairo University, Giza, Egypt.
[5]Electronics and Communications Engineering Dept., American University in Cairo, New Cairo, Egypt.
[6]Electrical Engineering Dept., Qatar University, Doha, Qatar.
adel@umn.edu, amr.elkeyi@sce.carleton.ca, {mohasseb, telbatt, mnafie}@ieee.org, kseddik@aucegypt.edu, tkhattab@ieee.org

***Abstract*—In this paper, we characterize the total degrees of freedom (DoF) of the full-duplex asymmetric multiple-input multiple- output (MIMO) 3-way channel. Each node has a separate-antenna full-duplex MIMO transceiver with a different number of antennas, where each antenna can be configured for either signal transmission or reception. We study this system under two message configurations; the first configuration is when each node has two unicast messages to be delivered to the two other nodes, while the second configuration is when each node has two unicast messages as well as one broadcast message to be delivered to the two other nodes. For each configuration, we first derive upper bounds on the total DoF of the system. Cut-set bounds in conjunction with genie-aided bounds are derived to characterize the achievable total DoF. Afterwards, we analytically derive the optimal number of transmit and receive antennas at each node to maximize the total DoF of the system, subject to the total number of antennas at each node. Finally, the achievable schemes for each configuration are constructed. The proposed schemes are mainly based on zero-forcing and null-space transmit beamforming. We show that the derived outer and inner bounds on the total DoF are tight for each message configuration.**

I. Introduction

Interference-limited wireless communication networks have been extensively investigated over recent years. Despite the fact that uncoordinated interference decreases the achievable data rates in wireless networks, novel paradigms have emerged to sagaciously harness interference and, hence, efficiently utilize the scarce spectrum and enhance the network performance.

Full-duplex systems have attracted a great deal of attention recently due to their potential benefits to significantly enhance the throughput and spectral efficiency of conventional half-duplex systems [2]. Existing wireless communication systems operate in either a time-division duplex or a frequency-division duplex mode to separate the downlink and uplink traffic. However, recent results from academia [3]–[10] and industry [11] have proposed various practical designs to implement in-band full-duplex radios by cancelling or suppressing the self-interference signal, generated during simultaneous transmission and reception, at the RF and baseband level. There are two possible methods of antenna interfacing for full-duplex MIMO transceivers; separate-antenna architecture [3]–[7], and shared-antenna architecture [8]–[10]. In separate-antenna architecture, each antenna is dedicated to either signal transmission or reception. In shared-antenna architecture, each antenna simultaneously transmits and receives signals on the same channel with the aid of a circulator that routes the transmitted signal from the TX signal chain to the antenna and the received signal on the antenna to the RX signal chain. Full-duplex systems are envisioned to have an enormous impact on the evolution of future 5G generations of wireless communication systems.

A. Related Work

Several works have been dedicated to study the DoF of wireless networks with full-duplex operation [12]–[14]. The capacity region of a full-duplex wireless network with relay nodes, feedback and cooperation is characterized in [12]. The authors in [13] investigate the achievable total DoF of cellular networks in which a base station has full-duplex operation to simultaneously communicate with half-duplex mobile stations. In [14], the authors study the DoF of full-duplex bidirectional interference networks with and without a MIMO relay.

The two-way communication channel was introduced in the seminal paper by Shannon [15]. The capacity regions of several multi-user two-way networks have been studied in [16]. The extension of the two-way channel to the case

The research work of A. M. Elmahdy and T. ElBatt was made possible by grants number NPRP 4-1034-2-385 and NPRP 5-782-2-322 from the Qatar National Research Fund, QNRF (a member of Qatar Foundation, QF). The research work of A. El-Keyi, M. Nafie and T. Khattab was made possible by grant number NPRP 7-923-2-344 from the QNRF. The statements made herein are solely the responsibility of the authors.

Part of this work has been published in preliminary form in the IEEE Information Theory Workshop (ITW), Cambridge, UK, Sept. 2016 [1].

This article has been accepted for publication in a future issue of this journal, but has not been fully edited. Content may change prior to final publication. Citation information: DOI 10.1109/TCOMM.2017.2664866, IEEE Transactions on Communications

of three nodes, i.e., the 3-way channel, has recently attracted much attention [17]–[19]. It is assumed that all nodes operate in a perfect full-duplex mode. Furthermore, there are six unicast messages to be exchanged among the nodes; each node is intended to exchange unicast messages with the other nodes simultaneously. The sum-capacity of the 3-way channel, that characterizes the DoF of the channel, is studied in [17] for the Gaussian channel model. It is shown that the sum-capacity is achievable within a gap of 2 bits. The achievable transmission strategy is to allow the two nodes with the strongest channel coefficient to communicate while leaving the third node silent.

The capacity region of the 3-way channel is considered for the linear shift deterministic channel model with reciprocal channel gains in [18]. Under this framework, the outer bounds of the 3-way channel are related to those of the linear shift deterministic Y-channel [20] through Δ-Y transformation, inspired from electrical circuit theory. The capacity achieving schemes are mainly based on multi-way relaying by signal alignment, interference neutralization and backward decoding.

The authors in [19] investigate the symmetric DoF of a MIMO 3-way channel with homogeneous antenna configurations; each node has M_T transmit antennas and M_R receive antennas. Cut-set bounds and genie-aided upper bounds are derived to characterize the symmetric total DoF of the channel. Then, the authors propose achievable schemes for the derived total DoF based on null-space beamforming and MIMO interference alignment.

B. Summary of Contributions

The main contribution of this paper is the characterization of the total DoF of a MIMO 3-way channel with heterogeneous antenna configurations. Each node has a separate-antenna full-duplex MIMO transceiver where each antenna can be configured to either transmit or receive, and the nodes have different numbers of antennas. It should be noted that the proposed system model is a generalized version of the symmetric model studied by Maier *et al.* in [19] where the total number of antennas of each node are the same, and each node has M_T transmit antennas and M_R receive antennas. Furthermore, we study this system under two message configurations; first, each node has two unicast messages to be delivered to the two other nodes, and, second, each node has two unicast messages as well as one broadcast message to be delivered to the two other nodes.

For each message configuration, we first derive upper bounds on the total DoF of the system in terms of M_{T_ℓ} and M_{R_ℓ}, where $\ell \in \{1,2,3\}$. Under the unicast message configuration, cut-set bounds in conjunction with genie aided bounds are utilized to characterize the achievable total DoF in this case. On the other hand, under the unicast and broadcast message configuration, the cut-set bounds are achievable. It should be noted that a broadcast message is considered as a desired message by all nodes and it is not treated as interference. Therefore, unlike the unicast message configuration, a broadcast message gives an additional degree of freedom and, hence, the cut-set bounds can be achieved in this case. Afterwards, we analytically derive the optimal number of transmit and receive antennas at each node to maximize the total DoF of the system, subject to the total number of antennas at each node. Finally, the achievable schemes for each configuration are constructed. The schemes are mainly based on zero-forcing and null-space beamforming. For each message configuration, we show that the derived outer and inner bounds on the total DoF are tight.

C. Paper Organization

The remainder of this paper is organized as follows. The system model and underlying assumptions are presented in Section II. Next, the upper bounds on the total DoF of the system, the optimal antenna allocation at each node, and the achievable schemes are derived in Section III when the system only features unicast messages, whereas they are derived in Section IV when the system features unicast as well as broadcast messages. Finally, the paper is concluded in Section V.

D. Notation

Lower and upper boldface letters are used to denote column vectors and matrices, respectively. $\mathbf{X}^T$, $\mathbf{X}^H$ and $\mathbf{X}^\dagger$ denote the transpose, the Hermitian transpose and the pseudo-inverse of $\mathbf{X}$, respectively. $\mathbf{I}_m$ is an $m \times m$ identity matrix, and $\mathbf{0}_{m\times n}$ is an $m \times n$ zero matrix. The sequence $(\mathbf{x}(1), \mathbf{x}(2), \ldots, \mathbf{x}(N))$ is denoted by $\mathbf{x}^N$. Let $h(\mathbf{x})$ denote the differential entropy of a random vector $\mathbf{x}$, and $I(\mathbf{x};\mathbf{y})$ denote the mutual information between two random vectors $\mathbf{x}$ and $\mathbf{y}$.

II. System Model

We consider the MIMO 3-node fully-connected interference network, a.k.a. the MIMO 3-way channel, depicted in Fig. 1. Each node has a separate-antenna full-duplex MIMO transceiver where each antenna can be configured for either signal transmission or reception. Node ℓ, where $\ell \in \mathcal{U} = \{1,2,3\}$, has M_ℓ antennas of which it utilizes M_{T_ℓ} antennas for signal transmission and M_{R_ℓ} antennas for signal reception, where $M_{T_\ell} + M_{R_\ell} = M_\ell$. The proposed asymmetric setting entails a different number of antennas at the different nodes. Henceforth, without loss of generality, we assume that $M_1 \geq M_2 \geq M_3$. Moreover, the signals as well as the channel coefficients are assumed to be complex-valued. Similar to [17]–[19], we assume that the nodes operate in a perfect full-duplex mode, i.e., each node can transmit and receive messages simultaneously and the effect of residual self-interference, imposed by the transmit antennas on the receive antennas within the same transceiver, is perfectly cancelled or suppressed. It is worth mentioning that recent research results indicate that the practical implementation of separate-antenna in-band full-duplex MIMO transceivers is becoming technologically feasible [3]–[7], [21].

The 3-way channel features two kinds of messages; unicast messages and broadcast messages. In other words, node i can send one or more of three independent messages; two unicast messages W_{ij} and W_{ik} to nodes j and k with rates R_{ij} and R_{ik}, respectively, and one broadcast message $W_{i,\mathrm{BC}}$

This article has been accepted for publication in a future issue of this journal, but has not been fully edited. Content may change prior to final publication. Citation information: DOI 10.1109/TCOMM.2017.2664866, IEEE Transactions on Communications

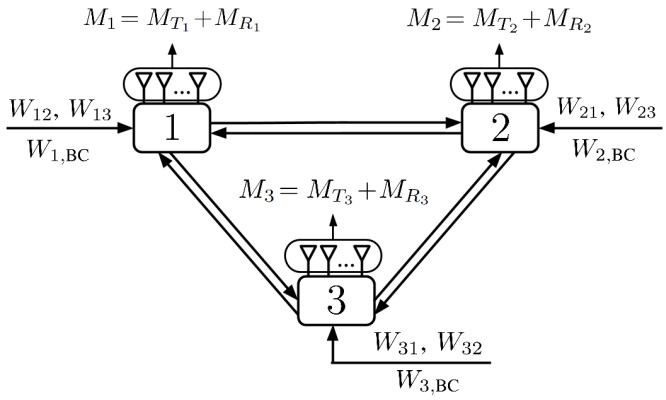

Fig. 1. The system model.

to both node j and node k with a rate $R_{i,\mathrm{BC}}$, for distinct $i, j, k \in \mathcal{U}$.

The transmitted signal from node i is denoted by $\mathbf{x}_i \in \mathbb{C}^{M_{T_i} \times 1}$. It is assumed that the power of the transmitted signal from node i is bounded by ρ, i.e., $\mathbb{E}\left\{\|\mathbf{x}_i\|^2\right\} \leq \rho$. Taking into account the aforementioned description of the system model, the received signal at node j at time slot n, denoted by $\mathbf{y}_j(n) \in \mathbb{C}^{M_{R_j} \times 1}$, is given by

$$\mathbf{y}_j(n) = \sum_{i \in \mathcal{U}, i \neq j} \mathbf{H}_{ij}\, \mathbf{x}_i(n) + \mathbf{z}_j(n)\,, \tag{1}$$

where $\mathbf{H}_{ij} \in \mathbb{C}^{M_{R_j} \times M_{T_i}}$ is the random channel matrix from node i to node j, and $\mathbf{z}_j \in \mathbb{C}^{M_{R_j} \times 1}$ is the additive noise signal at node j whose elements are independent and identically distributed (i.i.d.) complex Gaussian random variables with zero mean and unit variance. Throughout this paper, we assume that each node has perfect knowledge of the channel state information (CSI) from the two other nodes. Moreover, for the sake of notational simplicity, we drop the time index n throughout the sequel unless necessary.

Let $\mathbf{y}_\ell^n$ denote the sequence of $\mathbf{y}_\ell$ from time slot 1 up to time slot n, for $\ell \in \mathcal{U}$ and $n \in \mathcal{N}=\{1, 2, \ldots, N\}$. Now, we define the encoder and decoder functions for the considered system model [22]. The encoder function at node i maps its own messages W_{ij}, W_{ik} and $W_{i,\mathrm{BC}}$, and the past values of the received symbols $\mathbf{y}_i^{n-1}$ into the symbol $\mathbf{x}_i(n)$. Therefore, the encoder function $\mathcal{E}_i$ of node i is expressed as

$$\mathbf{x}_i(n) = \mathcal{E}_i\big(W_{ij}, W_{ik}, W_{i,\mathrm{BC}}, \mathbf{y}_i^{n-1}\big)\,, \tag{2}$$

for distinct $i, j, k \in \mathcal{U}$. On the other hand, for a transmission block of length N, the decoder function at node i maps its own messages W_{ij}, W_{ik} and $W_{i,\mathrm{BC}}$, and the received symbols in each block $\mathbf{y}_i^N$ to form estimates of its desired messages $\hat{W}_{ji}$, $\hat{W}_{ki}$, $\hat{W}_{j,\mathrm{BC}}$ and $\hat{W}_{k,\mathrm{BC}}$. Therefore, the decoder function $\mathcal{D}_i$ of node i is expressed as

$$\left(\hat{W}_{ji}, \hat{W}_{ki}, \hat{W}_{j,\mathrm{BC}}, \hat{W}_{k,\mathrm{BC}}\right) = \mathcal{D}_i\big(W_{ij}, W_{ik}, W_{i,\mathrm{BC}}, \mathbf{y}_i^N\big). \tag{3}$$

The capacity region of the full-duplex MIMO 3-way channel is the set of all achievable rate tuples $\mathcal{R}(\rho) = \{R_{12}(\rho)\,, R_{13}(\rho)\,, \ldots, R_{ij}(\rho)\,, R_{1,\mathrm{BC}}(\rho)\,, \ldots, R_{k,\mathrm{BC}}(\rho)\}$, for $i, j, k \in \mathcal{U}$ and $i \neq j$. The rates $R_{ij}(\rho) = \frac{\log |W_{ij}(\rho)|}{N}$ and $R_{k,\mathrm{BC}}(\rho) = \frac{\log |W_{k,\mathrm{BC}}(\rho)|}{N}$ are said to be achievable if the probability of error of all messages can be simultaneously made arbitrarily small when N is sufficiently large. In this work, we use the total DoF as the key performance metric to characterize the capacity behavior in the high signal-to-noise ratio (SNR) regime [23]. The DoF of a unicast message W_{ij} with a rate R_{ij} (as a function of the SNR) is designated as d_{ij}, for $i, j \in \mathcal{U}$ and $i \neq j$. It is characterized as

$$d_{ij} = \lim_{\mathrm{SNR} \to \infty} \frac{R_{ij}(\mathrm{SNR})}{\log(\mathrm{SNR})}. \tag{4}$$

Furthermore, the DoF of a broadcast message $W_{k,\mathrm{BC}}$ with a rate $R_{k,\mathrm{BC}}$ is designated as $d_{k,\mathrm{BC}}$, for $k \in \mathcal{U}$. It is characterized as

$$d_{k,\mathrm{BC}} = \lim_{\mathrm{SNR} \to \infty} \frac{R_{k,\mathrm{BC}}(\mathrm{SNR})}{\log(\mathrm{SNR})}. \tag{5}$$

The total DoF of the MIMO 3-way channel, d_Σ, is defined as

$$d_\Sigma = \sum_{i=1}^{3} \sum_{j=1, j \neq i}^{3} d_{ij} + 2 \sum_{k=1}^{3} d_{k,\mathrm{BC}}. \tag{6}$$

It should be noted that the DoF of broadcast messages is weighted by two since any broadcast message is desired by two nodes in the network [24]. In other words, the weighting factor of the DoF of a message represents the number of nodes that desires such a message and does not consider it as interference. Since each unicast message is desired by one node, and it is treated as interference by the other node, the DoF of unicast messages is weighted by one. On the contrary, each broadcast message is desired by two nodes and, hence, the DoF of broadcast messages is weighted by two.

III. Case I: Unicast Messages Only

In this section, we characterize the total DoF of the full-duplex asymmetric MIMO 3-way channel when only unicast messages are exchanged among the nodes. The following theorem presents the main result of this section.

Theorem 1. *The optimal total DoF of the MIMO 3-way channel, with $M_1 \geq M_2 \geq M_3$, where each node sends a unicast message to each of the two other nodes, is given by*

$$d_\Sigma = \min\left\{\frac{2M_1 + M_2 + M_3}{3},\ M_2 + M_3\right\}. \tag{7}$$

Proof: The converse proof of Theorem 1 is presented in Section III-A, together with the optimal antenna allocation at each node that can achieve the maximum total DoF of the system. Finally, the achievability proof of Theorem 1 is presented in Section III-B.

A. Converse Proof of Theorem 1

The proof is divided into three parts. First, the cut-set bounds are provided. Next, the genie-aided bounds are derived. Finally, the optimal antenna allocation at each node is derived in order to maximize the total DoF given by the cut-set and genie-aided bounds. Under the unicast communication scenario, the total DoF of the MIMO 3-way channel is characterized as

$$d_\Sigma = d_{12} + d_{13} + d_{21} + d_{23} + d_{31} + d_{32}. \tag{8}$$

This article has been accepted for publication in a future issue of this journal, but has not been fully edited. Content may change prior to final publication. Citation information: DOI 10.1109/TCOMM.2017.2664866, IEEE Transactions on Communications

*1) **Cut-set Bounds**:* The derivation of cut-set bounds hinges on the cut-set theorem [22]. Let $\mathcal{S}$ and $\mathcal{S}^c$ denote the set of source and destination nodes, respectively, where $\mathcal{S}^c$ is the complement of $\mathcal{S}$. We start the proof by arguing that the cooperation of any two nodes among the three nodes does not degrade the DoF [22]. Taking this fact into consideration, we first consider the cut around $\mathcal{S}=\{1\}$ and $\mathcal{S}^c=\{2,3\}$. This leads to the following inequality

$$d_{12}+d_{13} \leq \min\left\{M_{T_1},\ M_{R_2}+M_{R_3}\right\}. \tag{9}$$

Similarly, the following upper bounds can be obtained

$$d_{21}+d_{23} \leq \min\left\{M_{T_2},\ M_{R_1}+M_{R_3}\right\}, \tag{10}$$
$$d_{31}+d_{32} \leq \min\left\{M_{T_3},\ M_{R_1}+M_{R_2}\right\}. \tag{11}$$

Adding (9), (10) and (11), we get

$$\begin{aligned} d_{\Sigma} \leq \min\{&M_{T_1}+M_{T_2}+M_{T_3}, M_{T_1}+M_{T_2}+M_{R_1}+M_{R_2},\\ &M_{T_1}+M_{T_3}+M_{R_1}+M_{R_3}, M_{T_2}+M_{T_3}+M_{R_2}+M_{R_3},\\ &M_{T_1}+2M_{R_1}+M_{R_2}+M_{R_3}, M_{T_2}+M_{R_1}+2M_{R_2}+M_{R_3},\\ &M_{T_3}+M_{R_1}+M_{R_2}+2M_{R_3}, 2\left(M_{R_1}+M_{R_2}+M_{R_3}\right)\}. \end{aligned} \tag{12}$$

On the other hand, if we consider the cut around $\mathcal{S}=\{1,2\}$ and $\mathcal{S}^c=\{3\}$, we obtain

$$d_{13}+d_{23} \leq \min\left\{M_{T_1}+M_{T_2},\ M_{R_3}\right\}. \tag{13}$$

Similarly, the following upper bounds can be obtained

$$d_{21}+d_{31} \leq \min\left\{M_{T_2}+M_{T_3},\ M_{R_1}\right\}, \tag{14}$$
$$d_{12}+d_{32} \leq \min\left\{M_{T_1}+M_{T_3},\ M_{R_2}\right\}. \tag{15}$$

Adding (13), (14) and (15), we get

$$\begin{aligned} d_{\Sigma} \leq \min\{&M_{R_1}+M_{R_2}+M_{R_3}, M_{T_1}+M_{T_2}+M_{R_1}+M_{R_2},\\ &M_{T_1}+M_{T_3}+M_{R_1}+M_{R_3}, M_{T_2}+M_{T_3}+M_{R_2}+M_{R_3},\\ &M_{R_1}+2M_{T_1}+M_{T_2}+M_{T_3}, M_{R_2}+M_{T_1}+2M_{T_2}+M_{T_3},\\ &M_{R_3}+M_{T_1}+M_{T_2}+2M_{T_3}, 2(M_{T_1}+M_{T_2}+M_{T_3})\}. \end{aligned} \tag{16}$$

Combining (12) and (16), and then simplifying the resulting expression, the cut-set upper bound on the total DoF of the MIMO 3-way channel with unicast messages is characterized as

$$\begin{aligned} d_{\Sigma} \leq \min\{&M_{T_2}+M_{T_3}+M_{R_2}+M_{R_3},\ M_{T_1}+M_{T_2}+M_{T_3},\\ &M_{R_1}+M_{R_2}+M_{R_3}\}. \end{aligned} \tag{17}$$

In cut-set bounds, it is assumed that the nodes on the same side of the cut are fully cooperating. For instance, if we consider the cut around $\mathcal{S}=\{1\}$ and $\mathcal{S}^c=\{2,3\}$, we can imagine a genie that transfers W_{23} to node 3 and W_{32} to node 2. That is why, the cut-set bounds are referred to as the two-sided genie-aided bounds [25]. In order to establish tighter bounds on the total DoF, we resort to the one-sided genie-aided bounds [19], [25], [26] which we refer to as the genie-aided bounds in the sequel.

*2) **Genie-aided Bounds**:* The key idea of genie-aided bounds is that we assume the genie transfers the side-information from one node to another and not the other way around [25]. For example, in cut-set bounds, the genie transfers W_{23} and W_{32} to nodes 3 and 2, respectively. However, in genie-aided bounds, we assume that the genie transfers either W_{23} or W_{32} and, hence, the other message is not known at its respective node a priori.

We assume that every node can decode its desired unicast messages from the other nodes, according to the decoding function in (3), with an arbitrarily small probability of error. For example, node 1 decodes W_{21} and W_{31} using its received signal, $\mathbf{y}_1^N$, and its unicast messages, W_{12} and W_{13}, intended to node 2 and node 3, respectively. Thus, node 1 knows $\mathbf{y}_1^N$, W_{12}, W_{13}, W_{21} and W_{31} after the decoding process. Node 1 cannot decode more messages without being provided with additional side-information. In order to decode more messages, node 1 should be more knowledgeable than some other nodes. Suppose we want node 1 to be able to decode W_{32}. Knowing W_{21}, we should provide node 1 with W_{23} and $\mathbf{y}_2^N$ in order to decode W_{32}. Assume that the genie transfers W_{23} to node 1 as side-information. Then, what is left is to specifically know the additional side-information that is required to be transferred by the genie in order to generate $\mathbf{y}_2^N$. We will elaborate this as follows. Having W_{21} and W_{23}, node 1 can generate $\mathbf{x}_2(1)$. We then evaluate the following expression

$$\begin{aligned} \mathbf{y}_1(1)-\mathbf{H}_{21}\mathbf{x}_2(1) &= \mathbf{H}_{21}\mathbf{x}_2(1)+\mathbf{H}_{31}\mathbf{x}_3(1)+\mathbf{z}_1(1)-\mathbf{H}_{21}\mathbf{x}_2(1)\\ &= \mathbf{H}_{31}\mathbf{x}_3(1)+\mathbf{z}_1(1). \end{aligned} \tag{18}$$

Next, we multiply the previous expression by $\mathbf{H}_{31}^{\dagger}$ to get

$$\mathbf{H}_{31}^{\dagger}\left(\mathbf{y}_1(1)-\mathbf{H}_{21}\mathbf{x}_2(1)\right) = \mathbf{x}_3(1)+\mathbf{H}_{31}^{\dagger}\mathbf{z}_1(1). \tag{19}$$

It is worth mentioning that the left pseudo-inverse of $\mathbf{H}_{31}$ is guaranteed to exist almost surely if and only if $M_{R_1} \geq M_{T_3}$. Let us assume that this condition holds true for now and then we will later study the case when this condition is not satisfied. Taking into consideration Eq. (1), node 1 generates $\mathbf{y}_2(1)$ as follows.

$$\begin{aligned} &\mathbf{H}_{32}\left(\mathbf{x}_3(1)+\mathbf{H}_{31}^{\dagger}\mathbf{z}_1(1)\right)+\mathbf{H}_{12}\mathbf{x}_1(1)\\ &= \left(\mathbf{H}_{12}\mathbf{x}_1(1)+\mathbf{H}_{32}\mathbf{x}_3(1)+\mathbf{z}_2(1)\right)+\left(\mathbf{H}_{32}\mathbf{H}_{31}^{\dagger}\mathbf{z}_1(1)-\mathbf{z}_2(1)\right)\\ &= \mathbf{y}_2(1)+\mathbf{g}_{1,W_{23}}(1), \end{aligned} \tag{20}$$

where $\mathbf{g}_{1,W_{23}}(1) = \mathbf{H}_{32}\mathbf{H}_{31}^{\dagger}\mathbf{z}_1(1)-\mathbf{z}_2(1)$. We can see from (20) that the side-information that node 1 requires is $\mathbf{g}_{1,W_{23}}(1)$ and, hence, node 1 can subtract it from $\mathbf{H}_{32}\left(\mathbf{x}_3(1)+\mathbf{H}_{31}^{\dagger}\mathbf{z}_1(1)\right)+\mathbf{H}_{12}\mathbf{x}_1(1)$ to generate $\mathbf{y}_2(1)$. Having $\mathbf{y}_2(1)$, W_{21} and W_{23}, node 1 can generate $\mathbf{x}_2(2)$, according to the encoding function in (2). Following the same line of thought explained above, node 1 can accordingly generate $\mathbf{y}_2(2)$. Node 1 reiterates this procedure until it completely generates $\mathbf{y}_2^N$.

To sum up, when the genie transfers W_{23} as well as $\mathbf{g}_{1,W_{23}}^N$ to node 1 as side-information, it becomes more knowledgeable than node 2, that only has W_{21}, W_{23} and $\mathbf{y}_2^N$. Hence, node 1

This article has been accepted for publication in a future issue of this journal, but has not been fully edited. Content may change prior to final publication. Citation information: DOI 10.1109/TCOMM.2017.2664866, IEEE Transactions on Communications

can decode W_{32} in addition to W_{21} and W_{31}. From Fano's inequality, we can write

$$\begin{aligned}
&N\left(R_{21}+R_{31}+R_{32}\right)\\
&\leq I\left(\underbrace{W_{21},W_{31},W_{32}}_{W_1};\ \mathbf{y}_1^N,\underbrace{W_{12},W_{13},W_{23}}_{W_2},\mathbf{g}_{1,W_{23}}^N\right)+N\epsilon_N\\
&=I\left(W_1;\ \mathbf{y}_1^N,W_2,\mathbf{g}_{1,W_{23}}^N\right)+N\epsilon_N\\
&\overset{(a)}{=}I\left(W_1;\ W_2,\mathbf{g}_{1,W_{23}}^N\right)+I\left(W_1;\ \mathbf{y}_1^N\mid W_2,\mathbf{g}_{1,W_{23}}^N\right)+N\epsilon_N\\
&\overset{(b)}{=}I\left(W_1;\ \mathbf{y}_1^N\mid W_2,\mathbf{g}_{1,W_{23}}^N\right)+N\epsilon_N\\
&=h\left(\mathbf{y}_1^N\mid W_2,\mathbf{g}_{1,W_{23}}^N\right)-h\left(\mathbf{y}_1^N\mid W_1,W_2,\mathbf{g}_{1,W_{23}}^N\right)+N\epsilon_N\\
&\overset{(c)}{\leq}h\left(\mathbf{y}_1^N\right)-h\left(\mathbf{y}_1^N\mid W_1,W_2,\mathbf{g}_{1,W_{23}}^N\right)+N\epsilon_N\\
&\overset{(d)}{=}h\left(\mathbf{y}_1^N\right)-\sum_{n=1}^{N}h\left(\mathbf{y}_1(n)\mid\mathbf{y}_1^{n-1},W_1,W_2,\mathbf{g}_{1,W_{23}}^N\right)+N\epsilon_N\\
&\leq h\big(\mathbf{y}_1^N\big)-\sum_{n=1}^{N}h\big(\mathbf{y}_1(n)\mid\mathbf{y}_1^{n-1},W_1,W_2,\mathbf{g}_{1,W_{23}}^N,\dots\\
&\qquad\qquad\mathbf{y}_2^{n-1},\mathbf{y}_3^{n-1},\mathbf{x}_2^n,\mathbf{x}_3^n,\mathbf{z}_1^{n-1}\big)+N\epsilon_N\\
&\overset{(e)}{=}h\big(\mathbf{y}_1^N\big)-\sum_{n=1}^{N}h\big(\mathbf{z}_1(n)\mid\mathbf{y}_1^{n-1},W_1,W_2,\mathbf{g}_{1,W_{23}}^N,\dots\\
&\qquad\qquad\mathbf{y}_2^{n-1},\mathbf{y}_3^{n-1},\mathbf{x}_2^n,\mathbf{x}_3^n,\mathbf{z}_1^{n-1}\big)+N\epsilon_N\\
&\overset{(f)}{=}h\big(\mathbf{y}_1^N\big)-\sum_{n=1}^{N}h\big(\mathbf{z}_1(n)\mid\mathbf{g}_{1,W_{23}}^N,\mathbf{z}_1^{n-1}\big)+N\epsilon_N\\
&=h\big(\mathbf{y}_1^N\big)-h\big(\mathbf{z}_1^n\mid\mathbf{g}_{1,W_{23}}^N\big)+N\epsilon_N\\
&\leq\sum_{n=1}^{N}h\left(\left[\,\mathbf{H}_{21}\mathbf{H}_{31}\right]\begin{bmatrix}\mathbf{x}_2(n)\\ \mathbf{x}_3(n)\end{bmatrix}+\mathbf{z}_1(n)\right)+\mathcal{O}(1)+N\epsilon_N,
\end{aligned}\tag{21}$$

where $\mathcal{O}(1)$ is a term that is irrelevant to the DoF characterization, (a) follows from the chain rule for mutual information, (b) follows from the fact that W_1, W_2 and $\mathbf{g}_{1,W_{23}}^N$ are independent from each other and, hence, $I\left(W_1;\ W_2,\mathbf{g}_{1,W_{23}}^N\right)=0$, (c) follows from the fact that conditioning reduces entropy, (d) follows from the chain rule for entropy, (e) follows from the fact that $h\left(\mathbf{H}_{21}\,\mathbf{x}_2(n)+\mathbf{H}_{31}\,\mathbf{x}_3(n)+\mathbf{z}_1(n)\mid\mathbf{x}_2(n),\mathbf{x}_3(3)\right)=h\left(\mathbf{z}_1(n)\mid\mathbf{x}_2(n),\mathbf{x}_3(3)\right)$, and (f) follows from the fact that $\mathbf{z}_1(n)$ and $\left\{\mathbf{y}_i^{n-1},W_1,W_2,\mathbf{x}_j^n\right\}$ are independent, for $i\in\mathcal{U}$ and $j\in\mathcal{U}\backslash\{1\}$. It should be noted that $\epsilon_N\to0$ as $N\to\infty$. Thus, when $M_{R_1}\geq M_{T_3}$, the total DoF of W_{21}, W_{31} and W_{32} is upper bounded by

$$\begin{aligned}
N\left(d_{21}+d_{31}+d_{32}\right)&\leq N\left(\operatorname{rank}\left(\left[\,\mathbf{H}_{21}\mathbf{H}_{31}\,\right]\right)+\epsilon_N\right)\\
&=N\left(\min\{M_{R_1},M_{T_2}+M_{T_3}\}+\epsilon_N\right).
\end{aligned}\tag{22}$$

When dividing both sides by N and then letting $N\to\infty$, we obtain

$$d_{21}+d_{31}+d_{32}\leq\min\{M_{R_1},M_{T_2}+M_{T_3}\},\ \text{if}\ M_{R_1}\geq M_{T_3}.\tag{23}$$

On the other hand, when $M_{T_3}\geq M_{R_1}$, the left pseudo-inverse of $\mathbf{H}_{31}$ does not exist. To tackle this problem, we deduce an upper bound on the total DoF by increasing the number of receive antennas at node 1 such that $M_{R_1}=M_{T_3}$. As a result, the total DoF of W_{21}, W_{31} and W_{32} is upper bounded by

$$d_{21}+d_{31}+d_{32}\leq\min\{M_{T_3},M_{T_2}+M_{T_3}\},\ \text{if}\ M_{T_3}\geq M_{R_1}.\tag{24}$$

Combining (23) and (24), we finally get

$$d_{21}+d_{31}+d_{32}\leq\min\left\{\max\left\{M_{R_1},M_{T_3}\right\},M_{T_2}+M_{T_3}\right\}.\tag{25}$$

We have based our previous discussion on the assumption that the genie provides node 1 with W_{23} and $\mathbf{g}_{1,W_{23}}^N$ to be able to decode W_{32}. Now we assume that the genie transfers W_{32} and $\mathbf{g}_{1,W_{32}}^N$ to node 1 in order to decode W_{23}. Following the same approach, we can find that

$$\mathbf{g}_{1,W_{32}}^N=\mathbf{H}_{23}\mathbf{H}_{21}^{\dagger}\mathbf{z}_1^N-\mathbf{z}_3^N.\tag{26}$$

Therefore, the total DoF of W_{21}, W_{31} and W_{23} is upper bounded by

$$d_{21}+d_{31}+d_{23}\leq\min\left\{\max\left\{M_{R_1},M_{T_2}\right\},M_{T_2}+M_{T_3}\right\}.\tag{27}$$

Following the same procedure, we can derive the genie-aided bounds from node 2 and node 3 perspectives as follows. For node 2, when the genie provides it with W_{13} and $\mathbf{g}_{2,W_{13}}^N=\mathbf{H}_{31}\mathbf{H}_{32}^{\dagger}\mathbf{z}_2^N-\mathbf{z}_1^N$, the total DoF of W_{12}, W_{13} and W_{31} is upper bounded by

$$d_{12}+d_{32}+d_{31}\leq\min\left\{\max\left\{M_{R_2},M_{T_3}\right\},M_{T_1}+M_{T_3}\right\}.\tag{28}$$

On the other hand, when the genie provides node 2 with W_{31} and $\mathbf{g}_{2,W_{31}}^N=\mathbf{H}_{13}\mathbf{H}_{12}^{\dagger}\mathbf{z}_2^N-\mathbf{z}_3^N$, the total DoF of W_{12}, W_{13} and W_{13} is upper bounded by

$$d_{12}+d_{32}+d_{13}\leq\min\left\{\max\left\{M_{R_2},M_{T_1}\right\},M_{T_1}+M_{T_3}\right\}.\tag{29}$$

For node 3, when the genie provides it with W_{12} and $\mathbf{g}_{3,W_{12}}^N=\mathbf{H}_{21}\mathbf{H}_{23}^{\dagger}\mathbf{z}_3^N-\mathbf{z}_1^N$, the total DoF of W_{12}, W_{13} and W_{21} is upper bounded by

$$d_{13}+d_{23}+d_{21}\leq\min\left\{\max\left\{M_{R_3},M_{T_2}\right\},M_{T_1}+M_{T_2}\right\}.\tag{30}$$

On the other hand, when the genie provides node 3 with W_{21} and $\mathbf{g}_{3,W_{21}}^N=\mathbf{H}_{12}\mathbf{H}_{13}^{\dagger}\mathbf{z}_3^N-\mathbf{z}_2^N$, the total DoF of W_{12}, W_{13} and W_{12} is upper bounded by

$$d_{13}+d_{23}+d_{12}\leq\min\left\{\max\left\{M_{R_3},M_{T_1}\right\},M_{T_1}+M_{T_2}\right\}.\tag{31}$$

Adding (28) and (30), we obtain

$$\begin{aligned}
d_{\Sigma}\leq\min\{&2M_{T_1}+M_{T_2}+M_{T_3},M_{T_1}+M_{T_3}+\max\{M_{R_3},M_{T_2}\},\\
&M_{T_1}+M_{T_2}+\max\{M_{R_2},M_{T_3}\},\\
&\max\{M_{R_2},M_{T_3}\}+\max\{M_{R_3},M_{T_2}\}\}.
\end{aligned}\tag{32}$$

Adding (27) and (29), we get

$$\begin{aligned}
d_{\Sigma}\leq\min\{&M_{T_1}+M_{T_2}+2M_{T_3},M_{T_1}+M_{T_3}+\max\{M_{R_1},M_{T_2}\},\\
&M_{T_2}+M_{T_3}+\max\{M_{R_2},M_{T_1}\},\\
&\max\{M_{R_2},M_{T_1}\}+\max\{M_{R_1},M_{T_2}\}\}.
\end{aligned}\tag{33}$$

This article has been accepted for publication in a future issue of this journal, but has not been fully edited. Content may change prior to final publication. Citation information: DOI 10.1109/TCOMM.2017.2664866, IEEE Transactions on Communications

Adding (25) and (31), we obtain

$$\begin{aligned} d_\Sigma \leq \min\{&M_{T_1}+2M_{T_2}+M_{T_3}, M_{T_1}+M_{T_2}+\max\{M_{R_1}, M_{T_3}\}, \\ &M_{T_2}+M_{T_3}+\max\{M_{R_3}, M_{T_1}\}, \\ &\max\{M_{R_3}, M_{T_1}\}+\max\{M_{R_1}, M_{T_3}\}\}. \end{aligned} \tag{34}$$

Combining (32), (33) and (34) with the cut-set bounds given by (17), the total DoF of the MIMO 3-way channel with unicast messages is upper bounded by

$$\begin{aligned} d_\Sigma \leq \min\{&M_{T_1}+M_{T_2}+M_{T_3},\ M_{R_1}+M_{R_2}+M_{R_3}, \\ &\max\{M_{R_2}, M_{T_3}\}+\max\{M_{R_3}, M_{T_2}\}, \\ &\max\{M_{R_2}, M_{T_1}\}+\max\{M_{R_1}, M_{T_2}\}, \\ &\max\{M_{R_3}, M_{T_1}\}+\max\{M_{R_1}, M_{T_3}\}\}. \end{aligned} \tag{35}$$

Corollary 1. *The special case of $M_{T_1}=M_{T_2}=M_{T_3}=M_T$ and $M_{R_1}=M_{R_2}=M_{R_3}=M_R$, studied by Maier* et al. *in [19], is covered by* (35)*. In this case, the total DoF of the symmetric MIMO 3-way channel is upper bounded by*

$$d_\Sigma \leq \begin{cases} \min\{3M_R, 2M_T\} & \text{for } M_T \geq M_R, \\ \min\{3M_T, 2M_R\} & \text{for } M_T \leq M_R. \end{cases} \tag{36}$$

*3) **Optimal Antenna Allocation**:* In this part, we seek the optimal allocation of transmit and receive antennas at each node in terms of M_1, M_2 and M_3 to maximize the upper bound on the total DoF of the MIMO 3-way channel with unicast messages, given by (35). The optimization problem is formulated as follows

$$\begin{aligned} \textbf{P1:} \quad &\max_{d_\Sigma, M_{T_\ell}, M_{R_\ell}} d_\Sigma \\ &\text{s.t.} \quad (35), \\ &\quad M_{T_\ell}+M_{R_\ell}=M_\ell, \text{ for } \ell \in \{1,2,3\}. \end{aligned} \tag{37}$$

Lemma 1. *The total DoF of the MIMO 3-way channel with unicast messages only is upper bounded by*

$$d_\Sigma \leq d_\Sigma^\star, \tag{38}$$

*where $d_\Sigma^\star$ is the optimal solution of **P1**, which is given by*

$$d_\Sigma^\star = \begin{cases} \dfrac{2M_1+M_2+M_3}{3} & \text{for } M_1 \leq M_2+M_3 \\ M_2+M_3 & \text{for } M_1 \geq M_2+M_3. \end{cases} \tag{39}$$

When $M_1 \leq M_2+M_3$, one optimal antenna allocation that achieves the corresponding maximum total DoF is

$$\left[M_{R_1}^\star, M_{R_2}^\star, M_{R_3}^\star\right] = \left[0, \frac{M_1+2M_2-M_3}{3}, \frac{M_1+2M_3-M_2}{3}\right]. \tag{40}$$

On the other hand, when $M_1 \geq M_2+M_3$, one optimal antenna allocation that yields the maximum total DoF in this case is

$$\left[M_{R_1}^\star, M_{R_2}^\star, M_{R_3}^\star\right] = [M_2+M_3,\ 0,\ 0]. \tag{41}$$

*Note that $M_{T_\ell}^\star = M_\ell - M_{R_\ell}^\star$ according to the second constraint of **P1**.*

Proof: The details of the solution of **P1** are reported in Appendix A. This completes the converse proof of Theorem 1. ■

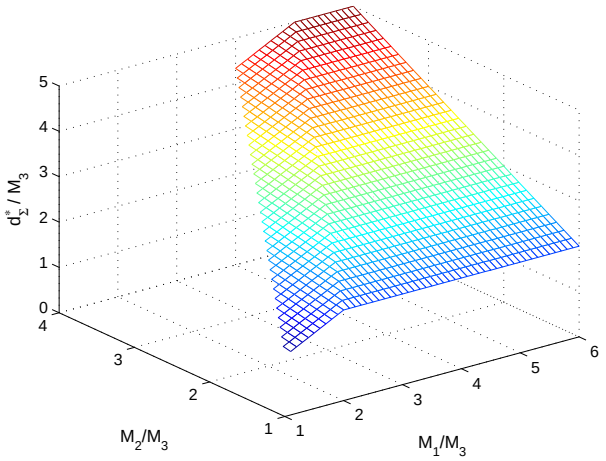

Fig. 2. The optimal total DoF of the full-duplex MIMO 3-way channel with unicast messages only, for $M_1 \geq M_2 \geq M_3$.

Fig. 2 depicts the optimal total DoF of **P1**. In the first region where $\frac{M_1}{M_3} \leq \frac{M_2}{M_3}+1$, the maximum total DoF is given by $\frac{1}{3}\left(\frac{2M_1}{M_3}+\frac{M_2}{M_3}+1\right)$. On the other hand, in the second region where $\frac{M_1}{M_3} \geq \frac{M_2}{M_3}+1$, the maximum total DoF is given by $\frac{M_2}{M_3}+1$.

B. Achievability Proof of Theorem 1

In this subsection, we provide the achievable schemes of total DoF of the MIMO 3-way channel described in Theorem 1. A message W_{ij} is encoded at the transmitter into the symbol $\mathbf{u}_{ij} \in \mathbb{C}^{r_{ij}\times 1}$, where $r_{ij} \leq M_{T_i}$. The transmitted signal from node i, $\mathbf{x}_i \in \mathbb{C}^{M_{T_i}\times 1}$, is defined as

$$\mathbf{x}_i = \mathbf{T}_{ij}\mathbf{u}_{ij} + \mathbf{T}_{ik}\mathbf{u}_{ik}, \text{ for distinct } i,j,k \in \mathcal{U}, \tag{42}$$

where $\mathbf{T}_{ij} \in \mathbb{C}^{M_{T_i}\times r_{ij}}$ is the precoding matrix for the signal transmitted from node i to node j.

1) $\boldsymbol{M_1 \leq M_2+M_3}$: In this case, the total DoF of the MIMO 3-way channel is bounded by $d_\Sigma \leq M_1 + \frac{M_2+M_3-M_1}{3}$. The transmit and receive antennas at each node are allocated as follows

$$\begin{aligned} M_{T_1} &= M_1, & M_{R_1} &= 0, \\ M_{T_2} &= \frac{M_2+M_3-M_1}{3}, & M_{R_2} &= \frac{M_1+2M_2-M_3}{3}, \\ M_{T_3} &= \frac{M_2+M_3-M_1}{3}, & M_{R_3} &= \frac{M_1+2M_3-M_2}{3}. \end{aligned} \tag{43}$$

It should be noted that if M_{T_ℓ} and M_{R_ℓ}, for $\ell \in \mathcal{U}$, are not integers, we use the symbol extension method over multiple time slots [27]. Then, we proceed with the design of the transmit strategy as explained below. Moreover, we assume in this achievable scheme that the number of antennas at each node is large enough to allow the allocation of transmit and receive antennas at the same time, i.e., $M_\ell \geq 3$ for $\ell \in \mathcal{U}$. For example, if $M_2 = 1$, the proposed achievable scheme cannot be applied since this number of antennas cannot be partitioned, by any means, to allow simultaneous operation of the transmit and receive modes. On the other hand, if $M_2 = 4$, we can apply the symbol extension method over three time slots. In

This article has been accepted for publication in a future issue of this journal, but has not been fully edited. Content may change prior to final publication. Citation information: DOI 10.1109/TCOMM.2017.2664866, IEEE Transactions on Communications

this case, joint precoding is performed over the three time slots and the equivalent channel matrices consist of 3 diagonal blocks.

In the proposed scheme, all nodes transmit signals while nodes 2 and 3 receive signals. Note that all antennas at node 1 are dedicated to signal transmission. The transmitted signals from each node are

$$\begin{aligned}\mathbf{x}_1 &= \mathbf{T}_{12}\mathbf{u}_{12} + \mathbf{T}_{13}\mathbf{u}_{13},\\ \mathbf{x}_2 &= \mathbf{T}_{23}\mathbf{u}_{23},\\ \mathbf{x}_3 &= \mathbf{T}_{32}\mathbf{u}_{32},\end{aligned} \tag{44}$$

where the dimensions of encoded data symbols $\mathbf{u}_{12}$, $\mathbf{u}_{13}$, $\mathbf{u}_{23}$ and $\mathbf{u}_{32}$ are $(M_{T_1}-M_{R_3})\times 1$, $(M_{T_1}-M_{R_2})\times 1$, $M_{T_2}\times 1$ and $M_{T_3}\times 1$, respectively, whereas the dimensions of precoding matrices $\mathbf{T}_{12}$, $\mathbf{T}_{13}$, $\mathbf{T}_{23}$ and $\mathbf{T}_{32}$ are $M_{T_1}\times(M_{T_1}-M_{R_3})$, $M_{T_1}\times(M_{T_1}-M_{R_2})$, $M_{T_2}\times M_{T_2}$ and $M_{T_3}\times M_{T_3}$, respectively. Note that $\mathbf{T}_{21}=\mathbf{T}_{31}=\mathbf{0}$ since $M_{R_1}=0$. The precoding matrices $\mathbf{T}_{12}$ and $\mathbf{T}_{13}$ are designed such that

$$\begin{aligned}\mathbf{T}_{12} &\in \mathrm{null}\left(\mathbf{H}_{13}\right),\\ \mathbf{T}_{13} &\in \mathrm{null}\left(\mathbf{H}_{12}\right).\end{aligned} \tag{45}$$

It is worth mentioning that the right pseudo-inverses of $\mathbf{H}_{13}$ and $\mathbf{H}_{12}$ exist almost surely owing to the fact that $M_{R_3}\leq M_{T_1}$ and $M_{R_2}\leq M_{T_1}$, respectively. On the other hand, the precoding matrices $\mathbf{T}_{23}$ and $\mathbf{T}_{32}$ are randomly selected. Consequently, the received signals at nodes 2 and 3 are

$$\begin{aligned}\mathbf{y}_2 &= \mathbf{H}_{12}\mathbf{T}_{12}\mathbf{u}_{12} + \mathbf{H}_{32}\mathbf{T}_{32}\mathbf{u}_{32} + \mathbf{z}_2,\\ \mathbf{y}_3 &= \mathbf{H}_{13}\mathbf{T}_{13}\mathbf{u}_{13} + \mathbf{H}_{23}\mathbf{T}_{23}\mathbf{u}_{23} + \mathbf{z}_3.\end{aligned} \tag{46}$$

Node 2 can decode $\mathbf{u}_{12}$ and $\mathbf{u}_{32}$ by projecting $\mathbf{y}_2$ to the null spaces of $\left(\mathbf{H}_{32}\mathbf{T}_{32}\right)^H$ and $\left(\mathbf{H}_{12}\mathbf{T}_{12}\right)^H$, respectively. Let $\mathbf{Q}_{12}\in\mathbb{C}^{M_{R_2}\times\left(M_{R_2}-M_{T_3}\right)}$ and $\mathbf{Q}_{32}\in\mathbb{C}^{M_{R_2}\times\left(M_{R_2}+M_{R_3}-M_{T_1}\right)}$ denote the projection matrices designed by node 2 such that

$$\begin{aligned}\mathbf{Q}_{12} &\in \mathrm{null}\left(\left(\mathbf{H}_{32}\mathbf{T}_{32}\right)^H\right),\\ \mathbf{Q}_{32} &\in \mathrm{null}\left(\left(\mathbf{H}_{12}\mathbf{T}_{12}\right)^H\right).\end{aligned} \tag{47}$$

Since we assume that the nodes have prefect CSI knowledge, the zero-forcing estimates of $\mathbf{u}_{12}$ and $\mathbf{u}_{32}$ at node 2 are

$$\begin{aligned}\hat{\mathbf{u}}_{12} &= \mathbf{G}_{12}\left(\mathbf{Q}_{12}^H\mathbf{H}_{12}\mathbf{T}_{12}\mathbf{u}_{12} + \mathbf{Q}_{12}^H\mathbf{z}_2\right),\\ \hat{\mathbf{u}}_{32} &= \mathbf{G}_{32}\left(\mathbf{Q}_{32}^H\mathbf{H}_{32}\mathbf{T}_{32}\mathbf{u}_{32} + \mathbf{Q}_{32}^H\mathbf{z}_3\right),\end{aligned} \tag{48}$$

where $\mathbf{G}_{12}\in\mathbb{C}^{\left(M_{T_1}-M_{R_3}\right)\times\left(M_{T_1}-M_{R_3}\right)}$ and $\mathbf{G}_{32}\in\mathbb{C}^{M_{T_3}\times M_{T_3}}$ are the inverses of $\mathbf{Q}_{12}^H\mathbf{H}_{12}\mathbf{T}_{12}$ and $\mathbf{Q}_{32}^H\mathbf{H}_{32}\mathbf{T}_{32}$, respectively. $\mathbf{G}_{12}$ and $\mathbf{G}_{32}$ are full rank almost surely because $\mathbf{Q}_{12}$ and $\mathbf{Q}_{32}$ are designed independently of $\mathbf{H}_{12}$ and $\mathbf{H}_{32}$, respectively, and $\mathbf{H}_{12}$ and $\mathbf{H}_{32}$ are drawn from a continuous random distribution. Similarly, node 3 can decode $\mathbf{u}_{13}$ and $\mathbf{u}_{23}$. As a result, node 2 decodes $M_{T_1}+M_{T_3}-M_{R_3}$ linearly independent information symbols while node 3 decodes $M_{T_1}+M_{T_2}-M_{R_2}$ linearly independent information symbols. Thus, the scheme achieves a total of $2M_{T_1}+M_{T_2}+M_{T_3}-M_{R_2}-M_{R_3}=\frac{2M_1+M_2+M_3}{3}$ DoF for $M_1\leq M_2+M_3$.

2) $\boldsymbol{M_1\geq M_2+M_3}$: In this case, the total DoF of the MIMO 3-way channel is bounded by $d_\Sigma\leq M_2+M_3$. The transmit and receive antennas at each node are allocated as follows

$$\begin{aligned}M_{T_1} &= M_1-(M_2+M_3), & M_{R_1} &= M_2+M_3,\\ M_{T_2} &= M_2, & M_{R_2} &= 0,\\ M_{T_3} &= M_3, & M_{R_3} &= 0.\end{aligned} \tag{49}$$

In the proposed scheme, nodes 2 and 3 transmit signals to node 1. The transmitted signals from nodes 2 and 3 are

$$\begin{aligned}\mathbf{x}_2 &= \mathbf{T}_{21}\mathbf{u}_{21},\\ \mathbf{x}_3 &= \mathbf{T}_{31}\mathbf{u}_{31},\end{aligned} \tag{50}$$

where $\mathbf{u}_{21}\in\mathbb{C}^{M_{T_2}\times 1}$ and $\mathbf{u}_{31}\in\mathbb{C}^{M_{T_3}\times 1}$, whereas $\mathbf{T}_{21}\in\mathbb{C}^{M_{T_2}\times M_{T_2}}$ and $\mathbf{T}_{31}\in\mathbb{C}^{M_{T_3}\times M_{T_3}}$. The precoding matrices $\mathbf{T}_{21}$ and $\mathbf{T}_{31}$ are randomly selected. The received signal at node 1 is

$$\mathbf{y}_1 = \mathbf{H}_{21}\mathbf{T}_{21}\mathbf{u}_{21} + \mathbf{H}_{31}\mathbf{T}_{31}\mathbf{u}_{31} + \mathbf{z}_1. \tag{51}$$

Analogous to the previous case, node 1 applies zero-forcing to decode $\mathbf{u}_{21}$ and $\mathbf{u}_{31}$ separately. In other words, node 1 can decode $\mathbf{u}_{21}$ and $\mathbf{u}_{31}$ by designing $\mathbf{V}_{21}$ and $\mathbf{V}_{31}$ such that $\mathbf{V}_{21}\in\mathrm{null}\left(\left(\mathbf{H}_{31}\mathbf{T}_{31}\right)^H\right)$ and $\mathbf{V}_{31}\in\mathrm{null}\left(\left(\mathbf{H}_{21}\mathbf{T}_{21}\right)^H\right)$, respectively. Afterwards, the zero-forcing estimates of $\mathbf{u}_{21}$ and $\mathbf{u}_{31}$ are obtained via evaluating the expressions $\mathbf{V}_{21}^H\mathbf{y}_1$ and $\mathbf{V}_{31}^H\mathbf{y}_1$, respectively. As a result, node 1 decodes a total of $M_{T_2}+M_{T_3}$ independent information symbols are decoded and, hence, the scheme achieves M_2+M_3 DoF for $M_1\geq M_2+M_3$. This completes the achievability proof of Theorem 1. ■

IV. Case II: Unicast and Broadcast Messages

In this section, we characterize the total DoF of the full-duplex asymmetric MIMO 3-way channel when unicast and broadcast messages are exchanged among the nodes. The following theorem presents the main result of this section.

Theorem 2. *The optimal total DoF of the MIMO 3-way channel, with $M_1\geq M_2\geq M_3$, where each node sends a unicast message to each of the two other nodes and a broadcast message to all other nodes, is given by*

$$d_\Sigma = M_2+M_3. \tag{52}$$

Proof: The converse proof of Theorem 2 is presented in Section IV-A, together with the optimal antenna allocation at each node that can achieve the maximum total DoF of the system. Finally, the achievability proof of Theorem 2 is presented in Section IV-B.

A. *Converse Proof of Theorem 2*

The proof is divided into two parts. First, the cut-set bounds are provided. Second, the optimal antenna allocation at each node is derived in order to maximize the total DoF given by the cut-set bounds. Under the unicast and broadcast communication scenario, the total DoF of the MIMO 3-way channel is characterized by (6).

This article has been accepted for publication in a future issue of this journal, but has not been fully edited. Content may change prior to final publication. Citation information: DOI 10.1109/TCOMM.2017.2664866, IEEE Transactions on Communications

*1) **Cut-set Bounds**:* Let us consider the cut around $\mathcal{S} = \{1,2\}$ and $\mathcal{S}^c = \{3\}$. This leads to the following inequality

$$d_{13}+d_{23}+d_{1,\text{BC}}+d_{2,\text{BC}} \leq \min\{M_{T_1}+M_{T_2},\ M_{R_3}\}. \quad (53)$$

Similarly, the following upper bounds can be obtained

$$d_{21}+d_{31}+d_{2,\text{BC}}+d_{3,\text{BC}} \leq \min\{M_{T_2}+M_{T_3},\ M_{R_1}\}, \quad (54)$$
$$d_{12}+d_{32}+d_{1,\text{BC}}+d_{3,\text{BC}} \leq \min\{M_{T_1}+M_{T_3},\ M_{R_2}\}. \quad (55)$$

Adding (53), (54) and (55), and then simplifying the resulting expression, the cut-set upper bound on the total DoF of the MIMO 3-way channel with unicast and broadcast messages is characterized as

$$d_\Sigma \leq \min\{M_{R_1}+M_{R_2}+M_{R_3}, M_{T_2}+M_{T_3}+M_{R_2}+M_{R_3}, M_{R_3}+M_{T_1}+M_{T_2}+2M_{T_3}, 2(M_{T_1}+M_{T_2}+M_{T_3})\}. \quad (56)$$

After finding the optimal antenna allocation at each node that maximizes the total DoF of the system, it will be shown in the achievability proof that the cut-set bounds are tight and can be achieved due to the presence of broadcast messages.

*2) **Optimal Antenna Allocation**:* In this part, we seek the optimal allocation of transmit and receive antennas at each node in terms of M_1, M_2 and M_3 to maximize the upper bound on the total DoF of the MIMO 3-way channel with unicast and broadcast messages, given by (56). The optimization problem is formulated as follows

$$\textbf{P2:} \quad \max_{d_\Sigma, M_{T_\ell}, M_{R_\ell}} d_\Sigma$$
$$\text{s.t.} \quad (56),$$
$$M_{T_\ell}+M_{R_\ell} = M_\ell, \ \text{for } \ell \in \{1,2,3\}. \quad (57)$$

Lemma 2. *The total DoF of the MIMO 3-way channel with unicast and broadcast messages is upper bounded by*

$$d_\Sigma \leq d_\Sigma^\star, \quad (58)$$

*where $d_\Sigma^\star$ is the optimal solution of **P2**, which is given by*

$$d_\Sigma^\star = M_2+M_3. \quad (59)$$

Furthermore, one optimal antenna allocation that achieves the maximum total DoF is

$$\left[M_{T_1}^\star, M_{T_2}^\star, M_{T_3}^\star\right] = [M_1-M_2,\ M_2-M_3,\ M_3]. \quad (60)$$

*Note that $M_{R_\ell}^\star = M_\ell - M_{T_\ell}^\star$ according to the second constraint of **P2**.*

Proof: The details of the solution of **P2** are reported in Appendix B. This completes the converse proof of Theorem 2. ∎

B. Achievability Proof of Theorem 2

In this subsection, we provide the achievable schemes of total DoF of the MIMO 3-way channel described in Theorem 2. In addition to unicast messages, a broadcast message $W_{i,\text{BC}}$ is encoded at the transmitter into the symbol $\mathbf{u}_{i,\text{BC}} \in \mathbb{C}^{r_{i,\text{BC}}\times 1}$, where $r_{i,\text{BC}} \leq M_{T_i}$. Accordingly, the transmitted signal from node i, $\mathbf{x}_i \in \mathbb{C}^{M_{T_i}\times 1}$, is defined as

$$\mathbf{x}_i = \mathbf{T}_{ij}\mathbf{u}_{ij}+\mathbf{T}_{ik}\mathbf{u}_{ik}+\mathbf{T}_{i,\text{BC}}\mathbf{u}_{i,\text{BC}}, \ \text{for distinct } i,j,k \in \mathcal{U}, \quad (61)$$

where $\mathbf{T}_{i,\text{BC}} \in \mathbb{C}^{M_{T_i}\times r_{i,\text{BC}}}$ is the broadcast precoding matrix of node i.

The total DoF of the MIMO 3-way channel is bounded by $d_\Sigma \leq M_2 + M_3$. The transmit and receive antennas at each node are allocated as follows

$$\begin{aligned} M_{T_1} &= M_1-M_2, & M_{R_1} &= M_2, \\ M_{T_2} &= M_2-M_3, & M_{R_2} &= M_3, \\ M_{T_3} &= M_3, & M_{R_3} &= 0. \end{aligned} \quad (62)$$

In the proposed scheme, nodes 2 and 3 transmit signals while nodes 1 and 2 receive signals. Note that all antennas at node 3 are utilized for signal transmission. The transmitted signals from nodes 2 and 3 are

$$\begin{aligned} \mathbf{x}_2 &= \mathbf{T}_{21}\mathbf{u}_{21}, \\ \mathbf{x}_3 &= \mathbf{T}_{3,\text{BC}}\mathbf{u}_{3,\text{BC}}, \end{aligned} \quad (63)$$

where $\mathbf{u}_{21} \in \mathbb{C}^{M_{T_2}\times 1}$ and $\mathbf{u}_{3,\text{BC}} \in \mathbb{C}^{M_{T_3}\times 1}$, whereas $\mathbf{T}_{21} \in \mathbb{C}^{M_{T_2}\times M_{T_2}}$ and $\mathbf{T}_{3,\text{BC}} \in \mathbb{C}^{M_{T_3}\times M_{T_3}}$ which are selected randomly. It is worth mentioning that $\mathbf{u}_{3,\text{BC}}$ is considered as a desired information symbol for nodes 1 and 2. Therefore, it is not treated as interference by either node. That is why, unlike unicast messages, broadcast messages provide additional degrees of freedom so that the cut-set bounds are tight and can be achieved. The received signal at nodes 1 and 2 are

$$\begin{aligned} \mathbf{y}_1 &= \mathbf{H}_{21}\mathbf{T}_{21}\mathbf{u}_{21} + \mathbf{H}_{31}\mathbf{T}_{3,\text{BC}}\mathbf{u}_{3,\text{BC}} + \mathbf{z}_1, \\ \mathbf{y}_2 &= \mathbf{H}_{32}\mathbf{T}_{3,\text{BC}}\mathbf{u}_{3,\text{BC}} + \mathbf{z}_2. \end{aligned} \quad (64)$$

Node 2 can decode $\mathbf{u}_{3,\text{BC}}$ using zero-forcing since $M_{R_2} = M_{T_3}$. On the other hand, node 1 separates $\mathbf{u}_{21}$ from $\mathbf{u}_{3,\text{BC}}$ by designing the zero-forcing matrices $\mathbf{V}_{21}$ and $\mathbf{V}_{3,\text{BC}}$ of $M_{R_1}\times(M_{R_1}-M_{T_3})$ and $M_{R_1}\times(M_{R_1}-M_{T_2})$ dimensions, respectively, such that

$$\begin{aligned} \mathbf{V}_{21} &\in \text{null}\left((\mathbf{H}_{31}\mathbf{T}_{3,\text{BC}})^H\right), \\ \mathbf{V}_{3,\text{BC}} &\in \text{null}\left((\mathbf{H}_{21}\mathbf{T}_{21})^H\right). \end{aligned} \quad (65)$$

Therefore, the following filtered signals are obtained

$$\begin{aligned} \mathbf{V}_{21}^H\mathbf{y}_1 &= \mathbf{V}_{21}^H\mathbf{H}_{21}\mathbf{T}_{21}\mathbf{u}_{21} + \mathbf{V}_{21}^H\mathbf{z}_1, \\ \mathbf{V}_{3,\text{BC}}^H\mathbf{y}_1 &= \mathbf{V}_{3,\text{BC}}^H\mathbf{H}_{31}\mathbf{T}_{3,\text{BC}}\mathbf{u}_{3,\text{BC}} + \mathbf{V}_{3,\text{BC}}^H\mathbf{z}_1. \end{aligned} \quad (66)$$

As a result, node 1 decodes $M_{T_2}+M_{T_3}$ linearly independent information symbols, and node 2 decodes M_{T_3} linearly independent information symbols. Thus, the scheme achieves a total of $M_{T_2}+2M_{T_3} = M_2 + M_3$ DoF for $M_1 \geq M_2 \geq M_3$. This completes the achievability proof of Theorem 2. ∎

V. Conclusion

In this paper, we characterized the total DoF of a MIMO 3-way channel with an asymmetric number of antennas at the nodes. Each node has a separate-antenna full-duplex MIMO

transceiver where each antenna can be configured for either signal transmission or reception. In the first message configuration, we considered the unicast communication scenario where each node can send two unicast messages to the two other nodes. The achievable total DoF is characterized using cut-set as well as genie-aided bounds. We rigorously derived the genie-aided bounds for the system in order to tighten the bounds given by the cut-set theorem. In the second message configuration, we considered the unicast and broadcast communication scenario where each node can send two unicast messages as well as one broadcast message to the two other nodes. Due to the presence of broadcast messages, the cut-set bounds are tight and can be achieved. Next, we analytically derived the optimal allocation of transmit and receive antennas at each node in order to obtain the maximum total DoF for each message configuration, subject to the total number of antennas at each node. Finally, we constructed the achievable schemes for each configuration using zero-forcing and null-space beamforming techniques. For each message configuration, it is shown that the derived outer and inner bounds on the total DoF are tight.

APPENDIX A

In this appendix, we solve the optimization problem **P1** in (37). This problem is non-convex due to the non-convexity of the feasible set. In order to find the optimal solution of **P1**, we divide the non-convex feasible set into 2^6 polyhedrons, i.e., 2^6 convex subsets, and then maximize the objective function over each subset. The optimal solution of **P1** is obtained by selecting the solution that achieves the maximum value of the objective function among all the subproblems. We can further reduce the number of subproblems to half, i.e., to 2^5 subproblems, by observing the symmetry of the objective function and the feasible set of **P1** in $[M_{T_1}, M_{T_2}, M_{T_3}]$ and $[M_{R_1}, M_{R_2}, M_{R_3}]$, which can be readily verified as follows. Let $\left\{d_\Sigma^\star, M_{T_1}^\star, M_{T_2}^\star, M_{T_3}^\star, M_{R_1}^\star, M_{R_2}^\star, M_{R_3}^\star\right\}$ be the optimal solution of **P1**. Substituting with $M_{T_1} = M_{R_1}^\star$, $M_{T_2} = M_{R_2}^\star$, $M_{T_3} = M_{R_3}^\star$, $M_{R_1} = M_{T_1}^\star$, $M_{R_2} = M_{T_2}^\star$ and $M_{R_3} = M_{T_3}^\star$ yields the same optimal value of the objective function while satisfying all the constraints of **P1**. By using the aforementioned approach, solving **P1** entails a one-dimensional line search with low complexity since the search space is finite and relatively small. First, let us rewrite **P1** as follows

$$\begin{aligned}
\textbf{P3:}\quad \max_{d_\Sigma, M_{T_\ell}, M_{R_\ell}} \quad & d_\Sigma \\
\text{s.t.} \quad & d_\Sigma \le M_{T_1}{+}M_{T_2}{+}M_{T_3}, \\
& d_\Sigma \le M_{R_1}{+}M_{R_2}{+}M_{R_3}, \\
& d_\Sigma \le \max\{M_{R_2}, M_{T_3}\}{+}\max\{M_{R_3}, M_{T_2}\}, \\
& d_\Sigma \le \max\{M_{R_2}, M_{T_1}\}{+}\max\{M_{R_1}, M_{T_2}\}, \\
& d_\Sigma \le \max\{M_{R_3}, M_{T_1}\}{+}\max\{M_{R_1}, M_{T_3}\}, \\
& M_{T_\ell}{+}M_{R_\ell} = M_\ell, \ \text{for } \ell \in \{1,2,3\}. \qquad (67)
\end{aligned}$$

It should be noted that the optimal solution of **P1** (and **P3**) relies on the values of M_1, M_2, and M_3, or more specifically, whether $M_1 \le M_2{+}M_3$ or $M_1 \ge M_2{+}M_3$. Therefore, we study each case separately.

A. $M_1 \le M_2 + M_3$

Let us consider one of the subproblems of **P3** and derive a closed-form expression of its optimal solution. For instance, let us assume that $M_{R_2} \ge M_{T_3}$, $M_{R_3} \ge M_{T_2}$, $M_{T_1} \ge M_{R_2}$, $M_{T_2} \ge M_{R_1}$, $M_{T_1} \ge M_{R_3}$ and $M_{T_3} \ge M_{R_1}$. Adding these assumptions to **P3** together with the constraint $M_1 \le M_2{+}M_3$, we get the following convex optimization problem

$$\begin{aligned}
\textbf{P4:}\quad \max_{d_\Sigma, M_{R_\ell}} \quad & d_\Sigma \\
\text{s.t.} \quad & d_\Sigma \le M_{R_2}{+}M_{R_3}, \\
& d_\Sigma \le M_1{+}M_2{-}M_{R_1}{-}M_{R_2}, \\
& d_\Sigma \le M_1{+}M_3{-}M_{R_1}{-}M_{R_3}, \\
& d_\Sigma \ge 0, \quad 0 \le M_{R_\ell} \le M_\ell, \ \text{for } \ell \in \{1,2,3\}, \\
& M_{R_2} \ge M_{T_3}, \ M_{R_3} \ge M_{T_2}, \\
& M_{T_1} \ge M_{R_2}, \ M_{T_2} \ge M_{R_1}, \\
& M_{T_1} \ge M_{R_3}, \ M_{T_3} \ge M_{R_1}, \\
& M_1 \le M_2{+}M_3. \qquad (68)
\end{aligned}$$

P4 can be expressed in the matrix form as follows

$$\begin{aligned}
\textbf{P5:}\quad \min_{\mathbf{v}} \quad & \mathbf{c}^T\mathbf{v} \\
\text{s.t.} \quad & \mathbf{A}\mathbf{v} \preceq \mathbf{b}, \qquad (69)
\end{aligned}$$

where $\mathbf{v} = [d_\Sigma, M_{R_1}, M_{R_2}, M_{R_3}]^T$, $\mathbf{c} = [-1, 0, 0, 0]^T$,

$$\mathbf{A} = \begin{bmatrix}
1 & 0 & -1 & -1 \\
1 & 1 & 1 & 0 \\
1 & 1 & 0 & 1 \\
0 & 1 & 0 & 0 \\
0 & 0 & 1 & 0 \\
0 & 0 & 0 & 1 \\
-1 & 0 & 0 & 0 \\
0 & -1 & 0 & 0 \\
0 & 0 & -1 & 0 \\
0 & 0 & 0 & -1 \\
0 & 0 & -1 & -1 \\
0 & 0 & -1 & -1 \\
0 & 1 & 1 & 0 \\
0 & 1 & 1 & 0 \\
0 & 1 & 0 & 1 \\
0 & 1 & 0 & 1 \\
0 & 0 & 0 & 0
\end{bmatrix}, \quad \mathbf{b} = \begin{bmatrix}
0 \\
M_1{+}M_2 \\
M_1{+}M_3 \\
M_1 \\
M_2 \\
M_3 \\
0 \\
0 \\
0 \\
0 \\
-M_3 \\
-M_2 \\
M_1 \\
M_2 \\
M_1 \\
M_3 \\
M_2{+}M_3{-}M_1
\end{bmatrix}. \qquad (70)$$

It is obvious that **P5** is a linear program. In order to find the optimal solution of **P5**, we establish the Lagrange dual problem of the primal problem as follows

$$\begin{aligned}
\textbf{P6:}\quad \max_{\boldsymbol{\lambda}} \quad & -\mathbf{b}^T\boldsymbol{\lambda} \\
\text{s.t.} \quad & \mathbf{A}^T\boldsymbol{\lambda} + \mathbf{c} = 0, \\
& \boldsymbol{\lambda} \succeq 0, \qquad (71)
\end{aligned}$$

where $\boldsymbol{\lambda} = [\lambda_1, \lambda_2, \ldots, \lambda_{16}]^T$. If we can find a feasible point for **P5** and **P6** such that strong duality holds, i.e., the duality gap of the primal dual feasible pair, $\mathbf{c}^T\mathbf{v} + \mathbf{b}^T\boldsymbol{\lambda}$, is zero, then $\mathbf{v}^\star$ is primal optimal, $\boldsymbol{\lambda}^\star$ is dual optimal, and $d_\Sigma^\star = -\mathbf{c}^T\mathbf{v}^\star = \mathbf{b}^T\boldsymbol{\lambda}^\star$ [28].

Next, let us assume that the 1st, 2nd, 3rd and 8th constraints of the primal problem (**P5**) are active, i.e., the inequality

This article has been accepted for publication in a future issue of this journal, but has not been fully edited. Content may change prior to final publication. Citation information: DOI 10.1109/TCOMM.2017.2664866, IEEE Transactions on Communications

constraints are satisfied with equality. Therefore, the primal problem reduces to a linear system of 4 equations and 4 unknowns and, hence, a feasible solution for the primal problem is obtained as

$$\mathbf{v}=\left[\frac{2M_1+M_2+M_3}{3}, 0, \frac{M_1+2M_2-M_3}{3}, \frac{M_1+2M_3-M_2}{3}\right]^T. \tag{72}$$

It is worth mentioning that this feasible solution yields

$$[M_{T_1}, M_{T_2}, M_{T_3}]=\left[M_1, \frac{M_2+M_3-M_1}{3}, \frac{M_2+M_3-M_1}{3}\right]. \tag{73}$$

It is evident that the non-negativity constraint on M_{T_2} and M_{T_3} is satisfied only when $M_1 \leq M_2+M_3$. On the other hand, when strong duality holds, complementary slackness condition states that the ith optimal Lagrange multiplier $\lambda_i^\star$ is zero unless the ith inequality constraint is active at the optimum [28]. Taking this fact into consideration, let us assume that only the 1^{st}, 2^{nd}, 3^{rd} and 8^{th} elements of $\boldsymbol{\lambda}$ are non-zero. Thus, the dual problem reduces to a linear system of 4 equations and 4 unknowns and, hence, a feasible solution for the dual problem is

$$[\lambda_1, \lambda_2, \lambda_3, \lambda_8] = \left[\frac{1}{3}, \frac{1}{3}, \frac{1}{3}, \frac{2}{3}\right]. \tag{74}$$

Note that the resulting $\boldsymbol{\lambda}$ satisfies the non-negativity constraint. For the obtained values of $\mathbf{v}$ and $\boldsymbol{\lambda}$, the corresponding duality gap is

$$\mathbf{c}^T\mathbf{v} + \mathbf{b}^T\boldsymbol{\lambda} = 0. \tag{75}$$

Therefore, the primal dual feasible pair $(\mathbf{v}^\star, \boldsymbol{\lambda}^\star)$ is optimal and, hence, the maximum total DoF and the optimal antenna allocation of the considered subproblem are given by (72).

Similarly, we can formulate and solve all the remaining subproblems. It turns out that the total DoF resulting from solving the aforementioned subproblem is the maximum value that can be attained from solving all the subproblems of **P1**. Moreover, due to the symmetry feature of **P1**, we can readily find the other optimal solution of **P1** that yields the same maximum total DoF and satisfies all the constraints. Thus, when $M_1 \leq M_2+M_3$, the optimal total DoF of **P1** is given by (39), and one optimal antenna allocation that achieves the maximum total DoF is given by (40).

B. $M_1 \geq M_2 + M_3$

Following the same approach used in the previous case, we can find the optimal solution of **P1** when $M_1 \geq M_2+M_3$. It can be shown that the optimal total DoF of **P1** is given by (39), and one optimal antenna allocation that achieves the maximum total DoF is given by (41). This completes the proof.

APPENDIX B

In this appendix, we solve the optimization problem **P2** in (57). To this end, we first rewrite **P2** as follows

$$\begin{aligned}\textbf{P7:}\quad \max_{d_\Sigma, M_{T_\ell}}\ & d_\Sigma \\ \text{s.t.}\ & d_\Sigma \leq M_1+M_2+M_3-M_{T_1}-M_{T_2}-M_{T_3}, \\ & d_\Sigma \leq M_2+M_3, \\ & d_\Sigma \leq M_3+M_{T_1}+M_{T_2}+M_{T_3}, \\ & d_\Sigma \leq 2M_{T_1}+2M_{T_2}+2M_{T_3}, \\ & d_\Sigma \geq 0,\ \ 0 \leq M_{T_\ell} \leq M_\ell,\ \text{for } \ell \in \{1,2,3\}.\end{aligned} \tag{76}$$

Next, let us consider the following optimization problem

$$\begin{aligned}\textbf{P8:}\quad \max_{d_\Sigma, M_{T_\ell}}\ & d_\Sigma \\ \text{s.t.}\ & 0 \leq d_\Sigma \leq M_2+M_3, \\ & \max\left\{d_\Sigma-M_3, \frac{d_\Sigma}{2}\right\} \leq \sum_{\ell=1}^{3} M_{T_\ell} \leq \sum_{\ell=1}^{3} M_\ell - d_\Sigma, \\ & 0 \leq M_{T_\ell} \leq M_\ell,\ \text{for } \ell \in \{1,2,3\},\end{aligned} \tag{77}$$

where the 2^{nd} constraint of **P8** is the result of combining the 1^{st}, 3^{rd} and 4^{th} constraints of **P7**. It can be readily shown that

$$d_\Sigma^\star = M_2+M_3. \tag{78}$$

Substituting (78) in the 2^{nd} and 3^{rd} constraints of **P8**, we get

$$\begin{aligned} & M_2 \ \leq\ M_{T_1}^\star+M_{T_2}^\star+M_{T_3}^\star \ \leq\ M_1. \\ & 0 \leq M_{T_\ell}^\star \leq M_\ell,\ \text{for } \ell \in \{1,2,3\}.\end{aligned} \tag{79}$$

Since **P2** and **P8** are equivalent optimization problems, the optimal total DoF of **P2** is given by (59). Furthermore, according to (79), there are many solutions of **P2** that optimally allocate the transmit and receive antennas at each node to achieve the maximum total DoF. One optimal antenna allocation, that satisfies the conditions in (79), is given by (60). This completes the proof.

REFERENCES

[1] A. M. Elmahdy, A. El-Keyi, Y. Mohasseb, T. ElBatt, M. Nafie, and K. G. Seddik, "Asymmetric degrees of freedom of the full-duplex mimo 3-way channel," *IEEE Information Theory Workshop (ITW)*, pp. 469–473, Sept. 2016.

[2] A. Sabharwal, P. Schniter, D. Guo, D. W. Bliss, S. Rangarajan, and R. Wichman, "In-band full-duplex wireless: Challenges and opportunities," *IEEE Journal on Selected Areas in Communications*, vol. 32, no. 9, pp. 1637–1652, Sept. 2014.

[3] M. Duarte and A. Sabharwal, "Full-duplex wireless communications using off-the-shelf radios: Feasibility and first results," *Asilomar Conference on Signals, Systems, and Computers*, pp. 1558–1562, Nov. 2010.

[4] E. Aryafar, M. A. Khojastepour, K. Sundaresan, S. Rangarajan, and M. Chiang, "MIDU: Enabling MIMO full duplex," *Proceedings of the ACM International Conference on Mobile Computing and Networking (MobiCom)*, pp. 257–268, Aug. 2012.

[5] M. Duarte, C. Dick, and A. Sabharwal, "Experiment-driven characterization of full-duplex wireless systems," *IEEE Transactions on Wireless Communications*, vol. 11, no. 12, pp. 4296–4307, Dec. 2012.

[6] M. Duarte, A. Sabharwal, V. Aggarwal, R. Jana, K. K. Ramakrishnan, C. W. Rice, and N. K. Shankaranarayanan, "Design and characterization of a full-duplex multiantenna system for WiFi networks," *IEEE Transactions on Vehicular Technology*, vol. 63, no. 3, pp. 1160–1177, Mar. 2014.

[7] E. Everett, A. Sahai, and A. Sabharwal, "Passive self-interference suppression for full-duplex infrastructure nodes," *IEEE Transactions on Wireless Communications*, vol. 13, no. 2, pp. 680–694, Feb. 2014.

[8] M. E. Knox, "Single antenna full duplex communications using a common carrier," *IEEE 13th Annual Wireless and Microwave Technology Conference (WAMICON)*, pp. 1–6, Apr. 2012.

[9] D. Bharadia, E. McMilin, and S. Katti, "Full duplex radios," *Proceedings of the ACM SIGCOMM*, pp. 375–386, Aug. 2013.

[10] S. Hong, J. Brand, J. I. Choi, M. Jain, J. Mehlman, S. Katti, and P. Levis, "Applications of self-interference cancellation in 5G and beyond," *IEEE Communications Magazine*, vol. 52, no. 2, pp. 114–121, Feb. 2014.

[11] "Kumu Networks," www.kumunetworks.com.

[12] V. R. Cadambe and S. A. Jafar, "Degrees of freedom of wireless networks with relays, feedback, cooperation, and full duplex operation," *IEEE Transactions on Information Theory*, vol. 55, no. 5, pp. 2334–2344, May 2009.

[13] S. H. Chae and S. H. Lim, "Degrees of freedom of cellular networks: Gain from full-duplex operation at a base station," *IEEE Global Communications Conference (GLOBECOM)*, pp. 4048–04053, Dec. 2014.

[14] Z. Cheng, N. Devroye, and T. Liu, "The degrees of freedom of full-duplex bidirectional interference networks with and without a mimo relay," *IEEE Transactions on Wireless Communications*, vol. 15, no. 4, pp. 2912–2924, Apr. 2016.

[15] C. E. Shannon, "Two-way communication channels," *4th Berkeley Symposium on Mathematical Statistics and Probability*, vol. 1, pp. 611–644, 1961.

[16] Z. Cheng and N. Devroye, "Two-way networks: When adaptation is useless," *IEEE Transactions on Information Theory*, vol. 60, no. 3, pp. 1793–1813, Mar. 2014.

[17] A. Chaaban, H. Maier, and A. Sezgin, "The degrees-of-freedom of multi-way device-to-device communications is limited by 2," *IEEE International Symposium on Information Theory (ISIT)*, pp. 361–365, Jul. 2014.

[18] H. Maier, A. Chaaban, R. Mathar, and A. Sezgin, "Capacity region of the reciprocal deterministic 3-way channel via Δ-Y transformation," 52^{nd} *Annual Allerton Conference on Communication, Control, and Computing (Allerton)*, pp. 167–174, Oct. 2014.

[19] H. Maier, A. Chaaban, and R. Mathar, "Symmetric degrees of freedom of the MIMO 3-way channel with $M_{\mathrm{T}} \times M_{\mathrm{R}}$ antennas," *IEEE Information Theory Workshop (ITW)*, pp. 92–96, Nov. 2014.

[20] A. Chaaban and A. Sezgin, "The capacity region of the linear shift deterministic Y-channel," *IEEE International Symposium on Information Theory (ISIT)*, pp. 2457–2461, Jul. 2011.

[21] S. Han, C.-L. I, Z. Xu, C. Pan, and Z. Pan, "Full duplex: Coming into reality in 2020?" *IEEE Global Communications Conference (GLOBECOM)*, pp. 4776–4781, Dec. 2014.

[22] T. M. Cover and J. A. Thomas, *Elements of Information Theory*, Wiley-Interscience, 2006.

[23] V. R. Cadambe and S. A. Jafar, "Interference alignment and degrees of freedom of the K-user interference channel," *IEEE Transactions on Information Theory*, vol. 54, no. 8, pp. 3425–3441, Aug. 2008.

[24] M. Salah, A. El-Keyi, M. Nafie, and Y. Mohasseb, "Achievable degrees of freedom on K-user MIMO multi-way relay channel with common and private messages," *Asilomar Conference on Signals, Systems, and Computers*, pp. 973–977, Nov. 2015.

[25] M. Mokhtar, Y. Mohasseb, M. Nafie, and H. El Gamal, "On the deterministic multicast capacity of bidirectional relay networks," *IEEE Information Theory Workshop (ITW)*, pp. 1–5, Aug. 2010.

[26] A. Chaaban, K. Ochs, and A. Sezgin, "The degrees of freedom of the MIMO Y-channel," *IEEE International Symposium on Information Theory (ISIT)*, pp. 1581–1585, Jul. 2013.

[27] S. A. Jafar and S. Shamai (Shitz), "Degrees of freedom region of the MIMO X channel," *IEEE Transactions on Information Theory*, vol. 54, no. 1, pp. 151–170, Jan. 2008.

[28] S. Boyd and L. Vandenberghe, *Convex Optimization*, Cambridge University Press, 2004.

Adel M. Elmahdy received the B.Sc. degree in electrical engineering from Alexandria University, Egypt, in 2011, and the M.Sc. degree in wireless communications from Nile University, Egypt, in 2015. He is currently pursuing the Ph.D. degree in electrical engineering with the University of Minnesota, Minneapolis, MN, USA. He was a Graduate Research Assistant and a Teaching Assistant with The American University in Cairo, Egypt, from 2011 to 2012. He joined the Wireless Intelligent Networks Center, Nile University, in 2013, as a Research Assistant. He was a Research Assistant with Qatar University, Qatar, from 2015 to 2016. He is a recipient of the Graduate Fellowship from Nile University in 2013 and 2014, and the ADC Fellowship from the University of Minnesota in 2016. His research interests include wireless communications, network coding, and multiuser information theory.

Amr El-Keyi received the B.Sc. (with highest honors) and M.Sc. degrees in Electrical Engineering from Alexandria University in 1999 and 2002, respectively, and the Ph.D. degree in 2006 in Electrical Engineering from McMaster University, Hamilton, ON, Canada. From November 2006 till April 2008, he was a postdoctoral research fellow with the Department of Electrical and Computer Engineering at McGill University. From May 2008 till February 2009, he was an Assistant Professor at Alexandria University where he participated in teaching several undergraduate courses. In April 2009, he joined Nile University as an Assistant Professor at the School of Communication and Information Technology and was promoted to Associate Professor in January 2015. His research interests include array processing, cognitive radio, channel estimation, interference management, and cooperative relaying for wireless communication systems. He has more than 70 refereed conference and journal publications.

Yahya Mohasseb (S' 98, M' 02, SM' 08) is a professor at the department of communications, the Military Technical College (MTC), Cairo, Egypt. He received both his Bachelor and Master degrees from MTC in 1991 and 1996 respectively, and his PhD from the Ohio State University in 2002, all in electrical engineering. Since then, he held several positions with the MTC including head of the educational affairs branch and head of the technical and engineering research center. He is currently head of the Electrical Engineering Branch. His technical and academic research interests include network information theory, multi-carrier communications, cognitive radio, software defined radio, multimedia security, channel modeling and estimation, satellite communications and Command & Control systems. Dr. Mohasseb is a recipient of the medal of duty and the medal of long service from the Egyptian MoD.

This article has been accepted for publication in a future issue of this journal, but has not been fully edited. Content may change prior to final publication. Citation information: DOI 10.1109/TCOMM.2017.2664866, IEEE Transactions on Communications

Tamer ElBatt received the B.S. and M.S. degrees in Electronics and Communications Engineering from Cairo University, Egypt, in 1993 and 1996, respectively, and the Ph.D. degree in Electrical and Computer Engineering from the University of Maryland, College Park, MD, USA in 2000. From 2000 to 2009 he was with major U.S. industry R&D labs, e.g., HRL Laboratories, LLC, Malibu, CA, USA and Lockheed Martin ATC, Palo Alto, CA, USA, at various positions. In July 2009, he joined the Electronics and Communications Dept., Faculty of Engineering, Cairo University, Egypt, as an Assistant Professor, where he is currently an Associate Professor. He also holds a joint appointment with Nile University, Egypt since Oct. 2009 and currently serves as the Director of the Wireless Intelligent Networks Center (WINC) since Oct. 2012. Dr. ElBatt research has been supported by the U.S.DARPA, ITIDA, QNRF, FP7,General Motors, Microsoft and Google and is currently being supported by NTRA, H2020 and Vodafone Egypt Foundation. He has published more than 95 papers in prestigious journals and international conferences. Dr. ElBatt holds seven issued U.S. patents.

Dr. ElBatt is a Senior Member of the IEEE and has served on the technical program committees of numerous IEEE and ACM conferences. He served as the Demos Co-Chair of ACM Mobicom 2013 and the Publications Co-Chair of IEEE Globecom 2012 and EAIMobiquitous 2014. Dr. ElBatt currently serves on the Editorial Board of IEEE Transactions on Mobile Computing and Wiley International Journal of Satellite Communications and Networking. Dr. ElBatt was a Visiting Professor at the Dept. of Electronics, Politecnico di Torino, Italy inAug. 2010, FENS, Sabanci University, Turkey in Aug. 2013and the Dept. of Information Engineering, University of Padova, Italy in Aug. 2015. Dr. ElBatt is the recipient of the 2014 Egypt's State Incentive Award in Engineering Sciences, the 2012 Cairo University Incentive Award in Engineering Sciences and the prestigious Google Faculty Research Award in 2011. His research interests lie in the broad areas of performance analysis, design and optimization of wireless and mobile networks.

Mohammed Nafie received his B.Sc. degree with honors from Cairo University in 1991. He received his M.Sc. degree with Distinction from King's College, University of London in 1993. He received his Ph.D. degree from University of Minnesota in 1999 where his research interests were in the area of low complexity detection algorithms. After his graduation he joined the Wireless Communications lab of the DSPS Research and Development Center of Texas Instruments. He was a primary contributor in TI's effort in the IEEE wireless personal area networks standardization process. In 2001, Dr. Nafie joined Ellipsis Digital Systems, where he was responsible for the development of the Physical Layer (PHY) of 802.11b wireless LAN standard. He has also participated in designing and optimizing the PHY of the 802.11a standard. In 2002, Dr. Nafie co-founded SySDSoft, a company specializing in the design of wireless digital communication systems. He was the Chief Technology Officer of SySDSoft till December 2006.

Dr. Nafie is currently a Professor at the Communications and Electronic Department of Cairo University, and at the Wireless Intelligent Networks Center of Nile University, for which he was a director from August 2009 to August 2012. His research interests are in the area of wireless and wireline digital communications and digital signal processing, and include equalization, LDPC coding, MIMO and relaying systems among others. Dr. Nafie has published numerous Journal and Conference papers, and has nineteen issued US patents as well as few others pending. He has several patents in Europe and Japan as well.

Karim G. Seddik (S' 04, M' 08, SM' 14) is an associate professor in the Electronics and Communications Engineering Department at the American University in Cairo (AUC), Egypt. Before joining AUC, he was an assistant professor in the Electrical Engineering Department at Alexandria University, Egypt. Dr. Seddik received the B.S. (with highest honors) and M.S. degrees in electrical engineering from Alexandria University, Alexandria, Egypt, in 2001 and 2004, respectively. He received his Ph.D. degree at the Electrical and Computer Engineering Department, University of Maryland, College Park 2008. His research interests include cooperative communications and networking, MIMO–OFDM systems, cognitive radio, layered channel coding, and distributed detection in wireless sensor networks.

Dr. Seddik has served on the technical program committees of numerous IEEE conferences in the areas of wireless networks and mobile computing. Dr. Seddik is a recipient of the Certificate of Honor from the Egyptian President for being ranked first among all departments in College of Engineering, Alexandria University in 2002, the Graduate School Fellowship from the University of Maryland in 2004 and 2005 and the Future Faculty Program Fellowship from the University of Maryland in 2007.

Tamer Khattab (M' 94) received his Ph.D. in Electrical and Computer Engineering from the University of British Columbia (UBC), Vancouver, BC, Canada in 2007, M.Sc. in Electronics and Communications Engineering and B.Sc. in Electronics and Communications Engineering from Cairo University, Giza, Egypt. Dr. Khattab joined Qatar University (QU) in 2007, where he is currently an associate professor of Electrical Engineering. He is also a senior member of the technical staff at Qatar Mobility Innovation Center (QMIC) an R&D center owned by QU and funded by Qatar Science and Technology Park (QSTP). Between 2006 and 2007 he was a postdoctoral fellow at the University of British Columbia working on prototyping advanced Gigabit/sec wireless LAN baseband transceivers. During 2000-2003 Dr. Khattab joined Alcatel Canada's Network and Service Management R&D in Vancouver, BC, Canada as a member of the technical staff working on development of core components for Alcatel 5620 network and service manager. Between 1994 and 1999 he was with IBM wtc. Egypt as a software development team lead working on development of several client-server corporate tools for IBM labs. Dr. Khattab's research interests cover physical layer transmission techniques in optical and wireless networks, information theoretic aspects of communication systems and MAC layer protocol design and analysis.